

RSC Advances



This article can be cited before page numbers have been issued, to do this please use: C. R.Rama, G. P. Geo, K.Rama Chandran, R. R. Chandran, A. T. Helen and G. K. George, *RSC Adv.*, 2015, DOI: 10.1039/C5RA11739A.



This is an *Accepted Manuscript*, which has been through the Royal Society of Chemistry peer review process and has been accepted for publication.

Accepted Manuscripts are published online shortly after acceptance, before technical editing, formatting and proof reading. Using this free service, authors can make their results available to the community, in citable form, before we publish the edited article. This *Accepted Manuscript* will be replaced by the edited, formatted and paginated article as soon as this is available.

You can find more information about *Accepted Manuscripts* in the [Information for Authors](#).

Please note that technical editing may introduce minor changes to the text and/or graphics, which may alter content. The journal's standard [Terms & Conditions](#) and the [Ethical guidelines](#) still apply. In no event shall the Royal Society of Chemistry be held responsible for any errors or omissions in this *Accepted Manuscript* or any consequences arising from the use of any information it contains.

Title : Design and development of $\text{Co}_3\text{O}_4/\text{NiO}$ composite nanofibers for the application of highly sensitive and selective non-enzymatic glucose sensors

Authors and Affiliations :

Author I :

Name : R. Ramachandran
Affiliation : Department of Physics and Nanotechnology, SRM University, Kattankulathur-603203, Tamil Nadu, India.

Author II :

Name : K. Ramachandran
Affiliation : Department of Physical Chemistry, School of Chemistry, Madurai Kamaraj University, Madurai-625021, India

Author III :

Name : Geo George Philip
Affiliation : Nanotechnology Research centre, SRM University, Kattankulathur-603203, Chennai, Tamil Nadu, India.

Author IV :

Name : Rasu Ramachandran
Affiliation : Department of Physical Chemistry, School of Chemistry, Madurai Kamaraj University, Madurai-625021, India

Author V:

Name : Helen Annal Therese
Affiliation : Nanotechnology Research centre, SRM University, Kattankulathur-603203, Chennai, Tamil Nadu, India.

Author VI :

Name : G.Gnana kumar
Affiliation : Department of Physical Chemistry, School of Chemistry, Madurai Kamaraj University, Madurai-625021, India

Corresponding Authors :

(I) Name : **Helen Annal Therese**
Affiliation : Nanotechnology Research centre, SRM University, Kattankulathur-603203, Chennai, Tamil Nadu, India.
E-mail : helen.a@ktr.srmuniv.ac.in

II) Name : **G.Gnana kumar**
Affiliation : Department of Physical Chemistry, School of Chemistry, Madurai Kamaraj University, Madurai-625021, India
Tel.No : 91-95857572997; E-mail : kumarg2006@gmail.com

Design and development of Co₃O₄/NiO composite nanofibers for the application of highly sensitive and selective non-enzymatic glucose sensors

R. Ramachandran,^a K. Ramachandran,^a Geo George Philip,^b Rasu Ramachandran,^a
Helen Annal Therese,^{*b} and G. Gnana kumar^{*c}

^a Department of Physics and Nanotechnology, SRM University, Kattankulathur-603 203, Tamil Nadu, India.

^b Nanotechnology Research centre, SRM University, Kattankulathur-603 203, Chennai, Tamil Nadu, India.

^c Department of Physical Chemistry, School of Chemistry, Madurai Kamaraj University, Madurai -625 021, Tamil Nadu, India.

Abstract

The cobaltic oxide/nickel oxide (Co₃O₄/NiO) composite nanofibers were synthesized *via* electrospinning technique and its electrocatalytic activities toward the non-enzymatic glucose sensors were evaluated in detail. Co₃O₄/NiO composite exhibited homogeneously distributed nanofibers with high porosity, effective inter connectivity and an extended number of conducting channels with an average diameter of 160 nm. The diffraction patterns depicted the face centred cubic crystalline structure of the Co₃O₄/NiO nanofibers and the purity of composite nanofibers was further ensured by using FT-IR and UV-*vis* spectroscopic analyses. The electrocatalytic performances of prepared nanofibers toward the oxidation of glucose was determined by cyclic voltammetry and amperometry techniques and the experimental results showed that the Co₃O₄/NiO composite nanofibers exhibited a maximum electrooxidation toward glucose, owing to the synergistic effect of Co₃O₄ and NiO. The electrospun Co₃O₄/NiO nanofibers exhibited a

detection limit of 0.17 μM , a wide linear range of 1 μM - 9.055 mM and a high sensitivity of 2477 $\mu\text{A mM}^{-1}\text{cm}^{-2}$. The nanofibers have also exhibited favorable properties such as good selectivity, reproducibility, durability and real sample analysis, which ensured its potential applications in the clinical diagnosis of diabetes.

Key words: conductive channels, electrospinning, nanofibers, oxidation, porosity.

*** Corresponding authors:**

* Helen Annal Therese: e.mail: helen.a@ktr.srmuniv.ac.in.

* G. Gnana kumar: e-mail: kumarg2006@gmail.com; Tel. No.: 919585752997.

1. Introduction

Diabetes is one of the most widespread diseases that affect the human population globally. Three hundred and eighty two million people are affected worldwide¹ and it causes 1.5 to 5.1 million deaths yearly, making it the 8th leading cause of death.² This pressing situation calls for the development of cheap, reliable and portable glucose sensors. Currently enzyme based/enzymatic glucose sensors are widely available on the market. Despite their widespread availability, there are some critical issues with enzymatic glucose sensors. The enzymatic glucose sensors are cost prohibitive, with prices reaching nearly 100 dollars per sensor.³ Apart from this, enzymatic glucose sensors suffer from poor reproducibility, thermal and chemical instabilities and susceptibility to enzyme poisoning molecules.^{4,5} The aforementioned serious problems with enzymatic glucose sensors have facilitated the need for alternate glucose sensors. A number of various methods such as colorimetry,⁶ fluorescent spectroscopy⁷ and other optical methods⁸ have been proposed; among which electrochemical non-enzymatic glucose sensors³ stand out. The affordable cost, low detection limits and high sensitivity of electrochemical based non-enzymatic glucose sensors favored their extensive applications.^{9,10} Hence, a large number of materials including precious¹¹⁻¹³ and non-precious metal^{14,15} and metal oxides^{16,17} have been tested for their suitability as non-enzymatic glucose sensor probes. Among these various metal and metal oxides, nickel (Ni) and nickel oxide (NiO) modified electrodes have shown very high sensitivity, low detection limits and good linear response toward glucose oxidation,¹⁸⁻²⁰ owing to its constructive properties such as large specific surface area, excellent electrical conductivity and better electrocatalytic activity. It also exhibits the advantage of being low cost due to the relative abundance of Ni in the earth's crust and NiO has shown to be superior over Ni due to the latter's tendency to get oxidized in air, which can drastically reduce its shelf life. However, pure NiO is

inevitably suffered by its poor surface stability under the oxidation conditions, leading to the poor sensitivity and selectivity.²¹ To effectively tackle this adverse impact, NiO based composites have received more attention, in which the impact of cobaltic oxide (Co_3O_4) is highly vibrant.²² If NiO is complexed with Co_3O_4 , the mechanical, chemical and electrochemical properties and structural stability of host material could be enhanced. Hence, the aforementioned metal oxide composites in the form of various morphologies such as nanorods²³, nanofibers²⁴ and as composites²⁵ have been shown to exhibit prompt sensitivity and selectivity toward glucose in the alkaline media.

One dimensional nanostructures such as nanofibers and nanorods have been shown to be effective sensor probes due to their larger surface to volume ratio and high porosity.^{26,27} One of the best methods to synthesize one dimensional porous nanostructures is the electrospinning technique. Electrospinning technique has the advantages of low cost, high yield and good reproducibility and it is a facile technique to produce porous and large surface to volume ratio nanofibers in large quantities.²⁸⁻³⁰ Electrospinning at the laboratory level can be easily scaled up to the industrial scale to meet the commercial requirements for the manufacture of non-enzymatic glucose sensors as opposed to conventional laboratory techniques such as sol-gel and hydrothermal methods. In general, the electrochemical quantification of glucose at prepared nanostructures is initiated by the adsorption, diffusion and followed by the oxidation at the catalyst's surface. The maximum electrooxidation is initiated by the effectual adsorption and diffusion processes, which can be stimulated only at the extended cavities/porosities of the prepared catalysts. The high porosity of electrospun nanofibers helps in trapping the analytes without any significant diffusion resistance, leading to an increase in the response to electroactive species,³¹ ensuring good sensitivity of the material toward glucose. To utilize the

advantages of nanofibers and metal oxide composites, $\text{Co}_3\text{O}_4/\text{NiO}$ composite nanofibers have been developed and its influences toward the electrooxidation of glucose under various electrochemical regimes and conditions have been analyzed and reported in this research effort.

2. Experimental methods

2.1. Materials

Polyvinyl alcohol (PVA) ($\text{MW} = 40,000 \text{ g mol}^{-1}$), nickel (II) acetate tetrahydrate ($\text{Ni}(\text{CH}_3\text{COO})_2 \cdot 4\text{H}_2\text{O}$), cobalt (II) nitrate hexahydrate ($\text{Co}(\text{NO}_3)_2 \cdot 6\text{H}_2\text{O}$), glacial acetic acid, N,N-dimethylformamide (DMF), glucose, urea (U), uric acid (UA), ascorbic acid (AA), dopamine (DA), acetaminophen (AP) and sodium chloride (NaCl) were obtained from Sigma-Aldrich and used without any further purification. All of these reagents were of analytical grade and used as received.

2.2. Preparation of PVA solution

For the preparation of 15 wt % PVA solution, an appropriate amount of PVA was dissolved in 10 ml of de-ionized water and the solution was stirred for 2 h at room temperature.

2.3. Preparation of $\text{Ni}(\text{CH}_3\text{COO})_2 \cdot 4\text{H}_2\text{O}$ solution

1M $\text{Ni}(\text{CH}_3\text{COO})_2 \cdot 4\text{H}_2\text{O}$ solution was added into 0.3 ml glacial acetic acid and magnetically stirred at room temperature. The glacial acetic acid was added to improve the conductivity of the electrospinning solution.

2.4. Preparation of $\text{Co}(\text{NO}_3)_2 \cdot 6\text{H}_2\text{O}$ solution

1 M $\text{Co}(\text{NO}_3)_2 \cdot 6\text{H}_2\text{O}$ solution was added into 0.3 ml glacial acetic acid and stirred at room temperature.

2.5. Preparation of PVA/(Co(NO₃)₂·6H₂O)/(Ni(CH₃COO)₂·4H₂O) and PVA/(Ni(CH₃COO)₂·4H₂O) solution

The equal quantities of 1 M Co(NO₃)₂·6H₂O and 1 M Ni(CH₃COO)₂·4H₂O solution were magnetically stirred for 30 min and one part of the Co(NO₃)₂·6H₂O/Ni(CH₃COO)₂·4H₂O solution was gradually added to the two parts of PVA solution and magnetically stirred for 30 min at room temperature to obtain a homogeneous solution. The PVA/Ni(CH₃COO)₂·4H₂O solution was prepared according to the same method.

2.6. Fabrication of electrospun nanofiber matrix

The prepared PVA/Co(NO₃)₂·6H₂O/Ni(CH₃COO)₂·4H₂O or PVA/Ni(CH₃COO)₂·4H₂O solution was transferred to the syringe. The distance from the needle to the drum collector was fixed at 18 cm and a voltage of 20 kV was applied to the tip of the nozzle. The flow rate of the syringe pump was set at 0.5 ml h⁻¹. The nanofibres were collected on the rotating drum collector set at a speed of 800 to 900 rpm. The electrospun nanofiber membrane was then collected and annealed in a muffle furnace to obtain the Co₃O₄/NiO composite nanofibers. The electrospun nanofiber membrane was annealed to 500 °C at a controlled rate of 2 °C min⁻¹ and the slow heating rate is critical to the proper formation of Co₃O₄/NiO nanofibers. The similar method was used for the synthesis of bare NiO nanofibers.

2.7. Modification of electrode

Before the surface modification of glassy carbon electrode (GCE) (3mm diameter), GCE was surface polished with 1.0, 0.3 and 0.05 μm alumina powder and then washed with de-ionized water, followed by sonication in ethanol and deionized water and dried at room temperature. The prepared nanofibers (2 mg ml⁻¹) were dispersed in a mixture of 0.02 ml Nafion and 0.18 ml DMF and the mixture was sonicated for 60 min to obtain a homogeneous dispersion. Then 10 μl of the

mixture was dropped onto the surface of polished GCE and dried at room temperature. The NiO and Co₃O₄/NiO nanofibers modified GCEs are represented as NiO/GCE and Co₃O₄/NiO/GCE, respectively.

2.8. Characterizations

The surface morphologies and average diameter of the nanofibers were investigated with a Field Emission - Scanning Electron Microscope (FE-SEM, FEG Quanta 200, FEI) coupled with Energy Dispersive X-Ray Spectroscopy analyzer (EDAX, Bruker) and Transmission Electron Microscope (TEM, JEOL 2010). The crystal structure of prepared nanofibers was investigated with a X-Ray Diffractometer (XRD, Xpert Pro, Panalytical). The Fourier transform infrared (FT-IR) transmission spectra of prepared nanofibers were obtained by employing a BRUKER α -Alpha-T Spectrometer with a SiC radiation source. The UV-*vis* absorption spectra of prepared nanofibers were acquired by using Metrohm (Analytical-Specord-220) spectroscopy.

2.9. Electrochemical characterizations

The electrochemical behavior of synthesized nanofibers were investigated by using a three electrode system, which consisted of a GCE, Ag/AgCl (1M KCl) and Pt wire as a working, reference and counter electrode, respectively. The electrochemical studies were carried out by using a CHI-650D electrochemical workstation at room temperature and the cyclic voltammograms (CV) and amperometric current responses were recorded by using the three electrode system. The electrocatalytic activity of modified electrodes was recorded in a solution containing 0.1 M NaOH at a scan rate of 20 mV s⁻¹ in the absence and presence of 1mM glucose by using cyclic voltammetry. The amperometric *i*-*t* measurements were carried out in a saturated 0.1 M NaOH solution with the successive addition of glucose solutions of different concentrations at an applied potential of 0.50 V vs. Ag/AgCl. The electroanalytical performances

of six bare/modified GCEs realized under the same conditions were evaluated and all of the electroanalytical performances were repeated for 4 times on each bare/modified GCEs and the average values were reported.

3. Results and Discussion

3.1. Morphological analysis

The surface morphological properties of PVA/Ni(CH₃COO)₂·4H₂O, PVA/Ni(CH₃COO)₂·4H₂O/Co(NO₃)₂·6H₂O, NiO and Co₃O₄/NiO nanofibers are provided in Fig. 1. The as-spun PVA/Ni(CH₃COO)₂·4H₂O (Fig. 1a) and PVA/Ni(CH₃COO)₂·4H₂O/Co(NO₃)₂·6H₂O nanofibers (Fig. 1b) exhibited smooth surfaces with the average fiber diameter of 325 nm and hundreds of micrometers in length. Even after the calcination process at 500 °C, the calcined samples maintained the nanofibrous morphologies. The average diameter of annealed fibers has shrunk to 160 nm for the bare NiO (Fig. 1c, d) and Co₃O₄/NiO nanofibers (Fig. 1e, f) and the reduction in the size of annealed nanofibers is attributed to the loss of polymer component during the annealing process. However, there were no significant changes observed in the length of prepared nanofibers. Furthermore, the smooth surface of fiber morphology was completely collapsed for the bare NiO (Fig. 1c,d) and Co₃O₄/NiO nanofibers (Fig. 1e,f), leading to the formation of a rough surface. The annealed nanofibers were composed of numerous nanograins with the relatively uniform distribution and average diameter of 25 nm. Both the bare NiO and Co₃O₄/NiO composite nanofibers exhibited a porous three dimensional network structure, which is expected to pave ways for the facile electron transportation for the excellent catalytic activity. The morphological properties of Co₃O₄/NiO composite nanofibers were further analyzed by using TEM (Fig. 1g) and it is clear that the resultant fiber is composed of uniformly

interconnected nanoparticles with an average diameter of 25 nm and the strong interconnection among the nanoparticles constructed the nanofiber morphology.

The existence of carbon and polymer residues in the nanofibers may interfere with the glucose sensing process. Hence, the aforementioned traces in bare NiO and Co₃O₄/NiO composite nanofibers were evaluated by using EDAX and the corresponding EDAX patterns are provided in Fig. 2. The presence of Ni and O elements in NiO nanofibers (Fig. 2a) and the existence of Ni, Co and O elements in Co₃O₄/NiO composite (Fig. 2b) ensured the chemical constituents of corresponding nanofibers. Although traces of carbon were found in both the NiO and Co₃O₄/NiO composite nanofibers, the traces are present in low amounts and can be considered as negligible.

3.2. Structural analysis

The diffraction patterns of prepared nanofibers are provided in Fig. 3 and NiO nanofibers exhibited the characteristic diffraction peaks at 38.2, 43.8, 63.2, 75.8 and 79.3 ° (Fig. 3a), which represent the (111), (200), (220), (311) and (222), respectively, reflection planes of a face centered single phase cubic NiO with the Fm-3m space group.³¹⁻³³ The diffraction patterns of electrospun composite nanofibers showed the formation of two separate phases - Co₃O₄ and NiO as illustrated in Fig. 3b and the reflection planes of Co₃O₄ and NiO correspond to the cubic crystal system with Fd-3m (JCPDS no. 01-078-1969) and Fm-3m space groups (JCPDS no. 01-071-1179), respectively.^{34,35} The peak broadening observed in the diffraction patterns specified the nanocrystalline structure of the grains in NiO and Co₃O₄/NiO composite nanofibers and the observed crystallite sizes are well matched with the morphological images. No other impurity phases observed from the XRD analysis ensured the structural purity of the prepared samples.

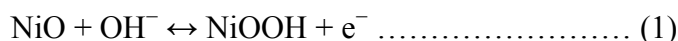
The structural characterizations of NiO and Co₃O₄/NiO composite nanofibers were further evaluated by using FT-IR and the corresponding spectra are provided in Fig. 4. The formation of NiO nanofibers (Fig. 4a) were ensured from the characteristic Ni-O stretching bands observed at 424, 451, 480 and 502 cm⁻¹.³⁶⁻³⁸ The spectrum corresponding to Co₃O₄/NiO composite nanofibers (Fig. 4b) exhibited all the Ni-O (420-500 cm⁻¹) stretching vibrations along with the new additional bands at 565 and 658 cm⁻¹. These additional bands correspond to the Co-O stretching vibrations of Co³⁺ and Co²⁺ present at the octahedral and tetrahedral sites of Co₃O₄ spinel, respectively.^{39, 40.}

The UV-*vis* spectroscopic analysis of NiO and Co₃O₄/NiO composite nanofibers were carried out over the wavelength of 200 - 800 nm and the obtained UV-*vis* spectra are shown in Fig. 5. A strong absorption band was observed at 320 nm (Inset: Fig. 5a) for the NiO nanofibers, owing to the electronic transition from the valence band to the conduction band of NiO.⁴¹ The UV-*vis* spectrum correspond to Co₃O₄/NiO composite nanofibers (Inset: Fig. 5b) exhibited a band at 320 nm, due to the Ni²⁺ transition. In addition, the two intra band transitions were observed in 700-850 nm and 450-600 nm ranges, which could be attributed to the lower and higher band gap charge transfer processes of Co³⁺ and Co²⁺ respectively.⁴² From the *tauc* plot drawn for both the nanofibers, it is clear that the band gap of Co₃O₄/NiO composite nanofibers is reduced to 2.19 eV from that of bare NiO nanofibers (3.87 eV).

3.3. Electrochemical performances

The electrochemical performances of bare GCE, NiO/GCE and Co₃O₄/NiO/GCE were characterized by using CV technique in 0.1 M NaOH in the potential range of -0.2 to 0.7 V at a scan rate of 20 mV s⁻¹ (Fig. 6a). The voltammograms obtained at bare GCE revealed that no noticeable redox behavior was observed, indicating that bare GCE was potentially silent under

the alkaline medium. However, the well defined redox peaks were obtained at both $\text{Co}_3\text{O}_4/\text{NiO}/\text{GCE}$ and NiO/GCE , owing to the presence of metal catalysts. The well-defined $\text{Ni}^{2+}/\text{Ni}^{3+}$ redox couple was obtained at NiO/GCE under an alkaline solution with the anodic (Epa) and cathodic (Epc) peak potential of +0.51 and +0.42 V vs. Ag/AgCl, respectively,^{43, 44} indicating that the prepared NiO nanofibers exhibited significant electrocatalytic activity in the alkaline medium and the involved electrochemical reaction is prescribed as follows:



The redox peak currents were further increased at $\text{Co}_3\text{O}_4/\text{NiO}/\text{GCE}$, owing to the higher catalytic activity of composite nanofibers through the synergetic effects of Co_3O_4 and NiO.^{45, 46} The generation of complex species at $\text{Co}_3\text{O}_4/\text{NiO}/\text{GCE}$ under alkaline conditions is identified from the Epa observed at 0.46 V vs. Ag/AgCl, which is intermediate between the NiO and Co_3O_4 anodic peak potentials. After the absorption of OH^- ions, both Ni^{2+} and Co^{2+} were transformed into Ni^{3+} and Co^{3+} respectively, and Co^{3+} was further oxidized into Co^{4+} at higher potentials. The Epc observed at 0.47 V vs. Ag/AgCl (Fig. 6a) is related with the reduction of Ni^{3+} and Co^{4+} formed in the positive scan and the involved reactions at $\text{Co}_3\text{O}_4/\text{NiO}/\text{GCE}$ are given below:

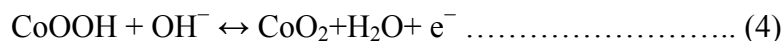
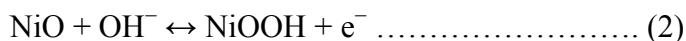
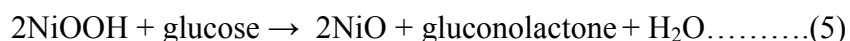


Fig. 6b shows the voltammograms of $\text{Co}_3\text{O}_4/\text{NiO}/\text{GCE}$ obtained in 0.1 M NaOH as a function of scan rate. It is clear that the anodic and cathodic peak responses were enhanced with the increasing scan rates ranging from 10 - 100 mV s^{-1} in 0.1 M NaOH. The anodic and cathodic peaks were shifted to positive and negative values, respectively; with the corresponding

increment in the scan rate. It is calculated that the I_p is proportional to the square root of scan rate with the high correlation coefficient (R) of 0.993 and 0.996 (Inset: Fig. 6b) for I_{pa} and I_{pc} , respectively; indicating that a diffusion-controlled quasi-reversible electrochemical reaction was occurred at $\text{Co}_3\text{O}_4/\text{NiO}/\text{GCE}$.

3.4. Electrocatalytic oxidation of glucose at GCE, NiO/GCE and $\text{Co}_3\text{O}_4/\text{NiO}/\text{GCE}$

The electro-oxidation of glucose at bare GCE, NiO/GCE and $\text{Co}_3\text{O}_4/\text{NiO}/\text{GCE}$ were examined by using CV technique under 1 mM glucose in 0.1 M NaOH at a scan rate of 20 mV s^{-1} and the obtained voltammograms are given in Fig. 7a. The bare GCE demonstrated negligible catalytic effects toward the glucose electro-oxidation in 0.1M NaOH in the potential window from -0.2 to +0.7 V. However, NiO/GCE has exhibited the prompt I_{pa} of $47 \mu\text{A}$ at +0.53 V *vs.* Ag/AgCl, which is ascribed to the electro-oxidation of glucose. It is well established that the observed I_{pa} is attributed to the electro-oxidation of glucose with the participation of Ni^{3+} centres in 0.1 M NaOH solution and the involved electrochemical reaction is given as follows:



The electrooxidation of glucose was further enhanced at $\text{Co}_3\text{O}_4/\text{NiO}/\text{GCE}$ as evidenced from the increased I_{pa} of $74 \mu\text{A}$ at 0.47 V *vs.* Ag/AgCl, indicating the irreversible maximum electrooxidation of glucose. The increased I_{pa} and positively shifted E_{pa} at $\text{Co}_3\text{O}_4/\text{NiO}/\text{GCE}$ than that of NiO/GCE are purely attributed to the effective participation of $\text{Ni}^{3+}/\text{Co}^{4+}$ centers of composite nanofibers generated at an alkaline medium.⁴⁷ The high porosity and well interconnected nanofibers were observed for the $\text{Co}_3\text{O}_4/\text{NiO}$ nanofibers. The free mobility of electrons throughout the length of nanofibers and extended number of electron transfer tunnels increased the delocalization of charges that enhanced the conductivity of prepared $\text{Co}_3\text{O}_4/\text{NiO}$ composite nanofibers. The cavities among the nanofibers and high porosity on the individual

nanofibers facilitated the rapid adsorption and followed by the efficient diffusion of an analyte glucose. The highly adsorbed glucose allowed the access of analytes to the catalytic active sites and facilitated the intimate contact between them with the minimal diffusion resistance. When the analyte glucose was rapidly diffused into the surface of electrode, it is oxidized into gluconolactone by the participation of $\text{Ni}^{3+}/\text{Co}^{4+}$ centres at $\text{Co}_3\text{O}_4/\text{NiO}/\text{GCE}$, leading to the increased I_{pa} under an alkaline solution. The increased electrooxidation of glucose observed at $\text{Co}_3\text{O}_4/\text{NiO}/\text{GCE}$ is ascribed to the synergistic effects of Co_3O_4 and NiO nanostructures that promoted the electrical conductivity and number of active sites. By the collective efforts afforded by the nanofibers and composite technologies, the maximum electrooxidation of glucose was observed at $\text{Co}_3\text{O}_4/\text{NiO}/\text{GCE}$ and the involved reaction mechanism is schematically illustrated in Fig. 7b.

Fig. 8a depicts the CVs of $\text{Co}_3\text{O}_4/\text{NiO}/\text{GCE}$ using different concentrations of glucose in 0.1M NaOH at a scan rate of 20 mV s^{-1} . The addition of glucose from 1 to 4 mM caused the obvious increase of I_{pa} with increasing glucose concentration without the potential shift. This phenomenon indicates the irreversible electrocatalysis of glucose under the positive scan and the catalytic conversion of Ni^{3+} and Co^{4+} to Ni^{2+} and Co^{3+} , respectively, under the negative scan. This result has exhibited the excellent electrocatalytic ability of $\text{Co}_3\text{O}_4/\text{NiO}/\text{GCE}$ in glucose oxidation and guarantees its amperometric glucose sensor applications.

Furthermore, the electrokinetics involved in $\text{Co}_3\text{O}_4/\text{NiO}/\text{GCE}$ was evaluated through different scan rates. Fig. 8b depicts the CVs of $\text{Co}_3\text{O}_4/\text{NiO}/\text{GCE}$ at different scan rates ($10\text{-}100 \text{ mV s}^{-1}$) using 1mM glucose in 0.1M NaOH. The E_{pa} and E_{pc} were slightly shifted to positive and negative values, respectively, with the corresponding increase in the scan rates. Moreover, the obtained I_{pa} and I_{pc} were linearly correlated to the square root of scan rates

(Inset: Fig. 8b) with the high correlation coefficient (R) of 0.992 (I_{pa}) and 0.995 (I_{pc}) respectively, implying that the reaction is a typical diffusion controlled electrochemical process.

3.5. Amperometric detection of glucose at $\text{Co}_3\text{O}_4/\text{NiO}/\text{GCE}$

Amperometric analysis is an extremely attractive technique, which is reflected by their fast response time toward the oxidation of glucose in the electrochemical sensor applications to evaluate the high sensitivity and detection limit toward glucose. The amperometric study was carried at $\text{Co}_3\text{O}_4/\text{NiO}/\text{GCE}$ with the successive step-wise addition of different concentrations of glucose in 0.1M NaOH at an applied potential of 0.5 V *vs.* Ag/AgCl (Fig. 9a). When the different concentration of glucose was added at a regular time intervals of 50 s into the alkaline medium, a rapid current increment was observed. The fast response and high values of the well-defined steady-state current response of non-enzymatic glucose sensor response toward glucose were observed. The steady state current has reached a fast response time of 6 s, owing to the excellent electrocatalytic activity, number of active sites, good electron mobility properties and inter connective network of $\text{Co}_3\text{O}_4/\text{NiO}$ nanofibers. Fig. 9b shows the calibration curve of the electrochemical response of $\text{Co}_3\text{O}_4/\text{NiO}/\text{GCE}$, which exhibited a wide linear range of glucose concentrations ranging from 1 μM to 9.055 mM with a high correlation coefficient of 0.998 ($n=27$). The fabricated $\text{Co}_3\text{O}_4/\text{NiO}/\text{GCE}$ exhibited the rapid response time, lower detection limit and high sensitivity of 5 s, 0.17 μM ($S/N=3$) and 2477 $\mu\text{A Mm}^{-1}\text{cm}^{-2}$, respectively. The obtained high sensitivity and low detection limit have been ascribed to the excellent electrocatalytic activity of the as-prepared $\text{Co}_3\text{O}_4/\text{NiO}$ nanofibers. The highly porous and three dimensional uniform network of $\text{Co}_3\text{O}_4/\text{NiO}$ nanofibers exhibited the large number of active sites. The porous three dimensional network has also permitted the easy access of glucose to the electrocatalytic active sites with the minimal diffusion resistance. The $\text{Co}_3\text{O}_4/\text{NiO}$ nanofibers

showed superior electrocatalytic activity toward non-enzymatic glucose sensing in comparison with the previous literatures as given in Table 1.⁴⁸⁻⁵⁹

3.6. Stability and reproducibility studies

To investigate the reproducibility of proposed system, six $\text{Co}_3\text{O}_4/\text{NiO}/\text{GCEs}$ were fabricated under the similar conditions and CV experiments were performed under the presence of 1 mM glucose. A relative standard deviation (RSD) of 3.32 % was obtained for a series of $\text{Co}_3\text{O}_4/\text{NiO}/\text{GCEs}$, specifying the good reproducibility of fabricated sensors. The operational stability of fabricated sensors was also monitored through the electro-oxidation of glucose for every 2 days for 30 days and $\text{Co}_3\text{O}_4/\text{NiO}/\text{GCE}$ was stored at inverted beaker at room temperature. It was found that the $\text{Co}_3\text{O}_4/\text{NiO}/\text{GCE}$ retained about 94.8 % of its original response to glucose oxidation after a month of storage, which indicates the good stability of the fabricated sensor system.

3.7. Interference studies

Interference test is the most significant technique in analytical methods, owing to the capability to distinguish the interfering species from the analyte, which have same physiological environment in the biosensor. U, UA, AA, DA, AP and NaCl are commonly used interfering species in the non-enzymatic electrochemical glucose sensors. Fig. 10 reveals the amperometric response at $\text{Co}_3\text{O}_4/\text{NiO}/\text{GCE}$ toward the addition of 1 mM glucose and 1 mM interfering species such as U, UA, AA, DA, AP and NaCl in 0.1 M NaOH at an applied potential of 0.5 V vs. Ag/AgCl. It is clear that $\text{Co}_3\text{O}_4/\text{NiO}/\text{GCE}$ has not exhibited any appreciable current response toward U, UA, AA, AP and NaCl. Although $\text{Co}_3\text{O}_4/\text{NiO}/\text{GCE}$ has exhibited a minimal current

response toward DA, the obtained current response is negligible in comparison with glucose. Thus the proposed sensor is accountable for good selectivity toward the detection of glucose.

3.8. Real sample analysis

The control of diabetic related diseases is purely dependent upon the tight monitoring of glucose in blood serum. Hence, the practical applicability of fabricated $\text{Co}_3\text{O}_4/\text{NiO}/\text{GCE}$ was evaluated with the 20 μl of human blood serum in 10 ml of 0.1 M NaOH (pH-13) solution and its amperometric current responses were monitored at an applied potential of 0.5 V vs. Ag/AgCl. The known concentrations of glucose were successively added into the blood serum and its corresponding electrochemical responses were noticed. The fabricated sensor exhibited an excellent recovery in the range of 97 – 104 % with the 2.67 – 3.36 % relative standard deviation (Table 2), which guaranteed the potential applications of proposed system in real samples.

The commercially available glucose monitoring systems are available at a cost of 60 to 100 US\$, which additionally requires the enzyme coated strips for evaluating the blood glucose levels and a strip costs between 0.45 to 1.0 US\$. Diabetic patients, who are prescribed insulin, need to check their blood glucose levels anywhere between 3 to 10 times in a day; constructing the blood glucose monitoring an expensive affair.⁶⁰ In contrast, the non-enzymatic sensor reported in this study requires approximately 30 μg of $\text{Co}_3\text{O}_4/\text{NiO}$ nanofibers and the maximum cost of the synthesis of nanofibers including high purity materials, electricity costs for electrospinning and calcination processes furnish a grand total of 0.15 US\$ per strip and the fabricated system can be reused for a couple of times without a drop in performance, which construct the feasible applications of proposed sensors at a large scale

4. Conclusion

The three dimensional network of $\text{Co}_3\text{O}_4/\text{NiO}$ composite nanofibers were synthesized *via* electrospinning and subsequent annealing processes. The electrospun nanofibers were highly porous, inter-connected and homogeneously distributed as seen from the morphological analysis and the prepared nanofibers were successively evaluated for its suitability as the non-enzymatic glucose sensor probes by using cyclic voltammetry and amperometric techniques. $\text{Co}_3\text{O}_4/\text{NiO}$ composite exhibited the superior electrooxidation toward glucose than that of bare NiO nanofibers and exhibited high sensitivity, wide linear range with low detection limit and has not been affected by the interferences. It has also demonstrated the high stability, excellent reproducibility and real sample analysis applications. The good analytical performance, low cost and facile preparation technique of the prepared electrospun composite $\text{Co}_3\text{O}_4/\text{NiO}$ nanofibers pave the ways for simple, effective and highly sensitive glucose biosensors. The fundamental issues provided in this report will be useful for the construction of on-site glucose sensors and thereby the diabetes can be controlled for the benefit of a healthy society.

Acknowledgment :

This work was supported by Council of Scientific and Industrial Research (CSIR), New Delhi, India, major Project Grant No.02(0060)/12/EMR-II.

References

- 1 Saunders in *Williams textbook of endocrinology*, Elsevier, Philadelphia, 12th edn., pp. 1371–1435.
- 2 S. P. Nichols, A. Koh, W. L. Storm, J. H. Shin, and M. H. Schoenfish, *Chem. Rev.*, 2013, 113, 2528.
- 3 G. Wang, X. He, L. Wang, A. Gu, Y. Huang, B. Fang, B. Geng and X. Zhang, *Microchim. Acta*, 2013, 180, 161.
- 4 X. H. Kang, Z. B. Mai, X. Y. Zou, P. X. Cai and J. Y. Mo, *Anal. Biochem.*, 2007, 363, 143.
- 5 X. Li, Q. Y. Zhu, S. F. Tong, W. Wang and W. B. Song, *Sens. Actuators B*, 2009, 136, 444.
- 6 M. Morikawa, N. Kimizuka, M. Yoshihara and T. Endo, *Chem. Eur. J.*, 2002, 8, 5580.
- 7 J. C. Pickup, F. Hussain, N. D. Evans, O. J. Rolinski and D. J. S. Birch, *Biosens. Bioelectron.*, 2005, 20, 2555.
- 8 S. Mansouri and J. S. Schultz, *Nat. Biotech.*, 1984, 2, 885.
- 9 D. Feng, F. Wang and Z. Chen, *Sens. Actuators B*, 2009, 138, 539.
- 10 X. Kang, Z. Mai, X. Zou, P. Cai and J. Mo, *Anal. Biochem.*, 2007, 363, 143.
- 11 Y. Bai, W. Yang, Y. Sun and Y. Sun, *Sens. Actuators B*, 2008, 134, 471.
- 12 S. Park, H. Boo and T. D. Chung, *Anal. Chim. Acta*, 2006, 556, 46.
- 13 M. Jia, T. Wang, F. Liang and J. Hu, *Electroanalysis*, 2012, 24, 1864.
- 14 Y. Zhang, L. Su, D. Manuzzi, H. V. E. Monteros, W. Jia, D. Huo, C. Hou and Y. Lei, *Biosens. Bioelectron.*, 2012, 31, 426.
- 15 C. Xia and W. Ning, *Electrochem. Commun.*, 2010, 12, 1581.
- 16 J. Wang, L. Wang, J. Di and Y. Tu, *Sens. Actuators B*, 2008, 135, 283.
- 17 F. Cao, S. Guo, H. Ma, G. Yang, S. Yang and J. Gong, *Talanta*, 2011, 86, 214.
- 18 A. Sun, J. Zheng and Q. Sheng, *Electrochim. Acta*, 2012, 65, 64.

- 19 B. Yuan, C. Xu, D. Deng, Y. Xing, L. Liu, H. Pang and D. Zhang, *Electrochim. Acta*, 2013, 88, 708.
- 20 Y. Mu, D. Jia, Y. He, Y. Miao and H. L. Wu, *Biosens. Bioelectron.*, 2011, 26, 2948.
- 21 J. Song, L. Xu, R. Xing, W. Qin, Q. Dai and H. Song, *Sens. Actuators B*, 2013, 182, 675.
- 22 L. Q. Qin, L. Y. Ming and L. J. Hong, *Chinese Sci. Bull.*, 2012, 57, 4195.
- 23 Chung-Wei Kung, Chia-Yu Lin, Yi-Hsuan Lai, R. Vittal and Kuo-Chuan Ho, *Biosens. Bioelectron.*, 2011, 27, 125.
- 24 Yu Ding, Ying Wang, Liang Su, Michael Bellagamba, Heng Zhang and Yu Lei, *Biosens. Bioelectron.*, 2010, 26, 542.
- 25 Xing-You Lang, Hong-Ying Fu, Chao Hou, Gao-Feng Han, Ping Yang, Yong-Bing Liu and Qing Jiang, *Nature Communications*, 2013, 4, 2169.
- 26 N. Senthilkumar, K. J. Babu, G. G. Kumar, A. R. Kim and D. J. Yoo, *Ind. Eng. Chem. Res.*, 2014, 53, 10347.
- 27 P. Gibson, H. S. Gibson and D. Rivin, *Colloids Surf., A*, 2001, 469, 187.
- 28 N. Bhardwaj and S. C. Kundu, *Biotechnol. Adv.*, 2010, 28, 325.
- 29 A. Greiner and J. H. Wendorff, *Angew. Chem., Int. Ed.*, 2007, 46, 5670.
- 30 D. Sabba, S. Agarwala, S. S. Pramana and S. Mhaisalkar, *Nanoscale Res. Lett.* 2014, 9, 14.
- 31 X. Su, J. Ren, X. Meng, X. Ren and F. Tang, *Analyst*, 2013, 138, 1459.
- 32 S. Vijayakumar, S. Nagamuthu and G. Muralidharan, *ACS Appl. Mater. Interfaces*, 2013, 5, 2188.
- 33 S. I. Kim, J. S. Lee, H. J. Ahn, H. K. Song and J. H. Jang, *ACS Appl. Mater. Interfaces* 2013, 5, 1596.

- 34 A. M. A. Enizi, A. A. Elzatahry, A. R. I. Soliman and S. S. A. Theyab, *Int. J. Electrochem. Sci.*, 2012, 7, 12646.
- 35 D. Malwal and P. Gopinath, *Environ. Sci.: Nano*, 2015, 2, 78.
- 36 P. S. Patil and L. D. Kadam, *Applied Surface Science*, 2002, 199, 211.
- 37 N. Dharmaraj, P. Prabu, S. Nagarajan, C.H. Kimb, J. H. Park and H.Y. Kimb, *Mat. Sci. Eng B*, 2006, 128, 111.
- 38 Yanping Wang, Junwu Zhu, Xujie Yang, Lude Lu and X. Wang, *Thermochimica Acta* 2005, 437, 106.
39. C. Nethravathi, S. Sen, N. Ravishankar, M. Rajamathi, C. Pietzonka and B. Harbrecht, *J. Phys. Chem. B*, 2005, 109, 11468.
- 40 Z. P. Xu and H. C. Zeng, *J. Mater. Chem.*, 1998, 8, 2499.
- 41 L. Wu, Y. Wu, H. Wei, Y. Shi and C. Hu, *Mater. Lett.* 2004, 58, 2700.
- 42 S. K. Meher and G. R. Rao, *J. Phys. Chem. C* 2011, 115, 25543.
- 43 Y. Mu, D. L. Jia, Y. Y. He, Y. Q. Miao and H.L. Wu, *Biosens. Bioelectron.*, 2011, 26, 2948.
- 44 X. H. Niu, M. B. Lan, H. L. Zhao and C. Chen, *Anal. Chem.*, 2013, 85, 3561.
- 45 K. Wang, Z. Zhang, X. Shi, H. Wang, Y. Lu and X. Ma, *RSC Adv.*, 2015, 5, 1943.
- 46 J. B. Wu, Z. G. Li, X. H. Huang and Y. Lin, *J. Power Sources*, 2013, 224, 1.
- 47 K. Xu, R. Zou, W. Li, Y. Xue, G. Song, Q. Liu, X. Liu and J. Hu, *J. Mater. Chem. A*, 2013, 1, 9107.
- 48 W. D. Zhang, J. Chen, L. C. Jiang, Y. X. Yu and J. Q. Zhang, *Microchim. Acta*, 2010, 168, 259.
- 49 W. Wang, L. Zhang, S. Tong, X. Li and W. Song, *Biosens. Bioelectron.*, 2009, 25, 708.

- 50 L Luo, F. Li, L. Zhu, Y. Ding, Z. Zhang, D. Deng and B. Lu, *Colloids Surf., B*, 2013, 102, 307.
- 51 X. Li, A. Hu, J. Jiang, R. Ding, J. Liu and X. Huang, *J. Solid State Chem.*, 2011, 184, 2738.
- 52 L. M. Lu, L. Zhang, F. L. Qu, H. X. Lu, X. B. Zhang, Z. S. Wu, S. Y. Huan, Q. A. Wang, G. L. Shen and R. Q. Yu, *Biosens. Bioelectron.*, 2009, 25, 218.
- 53 X. Li, J. Yao, F. Liu, H. He, M. Zhou, N. Mao, P. Xiao and Y. Zhang, *Sens. Actuators B*, 2013, 181, 501.
- 54 S. S. Mahshid, S. Mahshid, A. Dolati, M. Ghorbani, L. Yang, S. Luo and Q. Cai, *Electrochim. Acta*, 2011, 58, 551.
- 55 N. Q. Dung, D. Patil, H. Jung, J. Kim and D. Kim, *Sens. Actuators B*, 2013, 183, 381.
- 56 H. Nie, Z. Yao, X. Zhou, Z. Yang and S. Huang, *Biosens. Bioelectron.*, 2011, 30, 28.
- 57 54 Y. Ding, Y. Wang, L. Su, M. Bellagamba, H. Zhang and Y. Lei, *Biosens. Bioelectron.*, 2010, 26, 542.
- 58 S. Yu, X. Peng, G. Cao, M. Zhao, L. Qiao, J. Yao and H. He, *Electrochimica. Acta*, 2012, 76, 512.
- 59 W. Lu, X. Qin, A. M. Asiri, A. O. A. Youbi and X. Sun, *Analyst*, 2013, 138, 417.
- 60 S. F. Clarke, J. R. Foster, *Brit. J. Biomed. Sci.*, 2012, 69, 83.

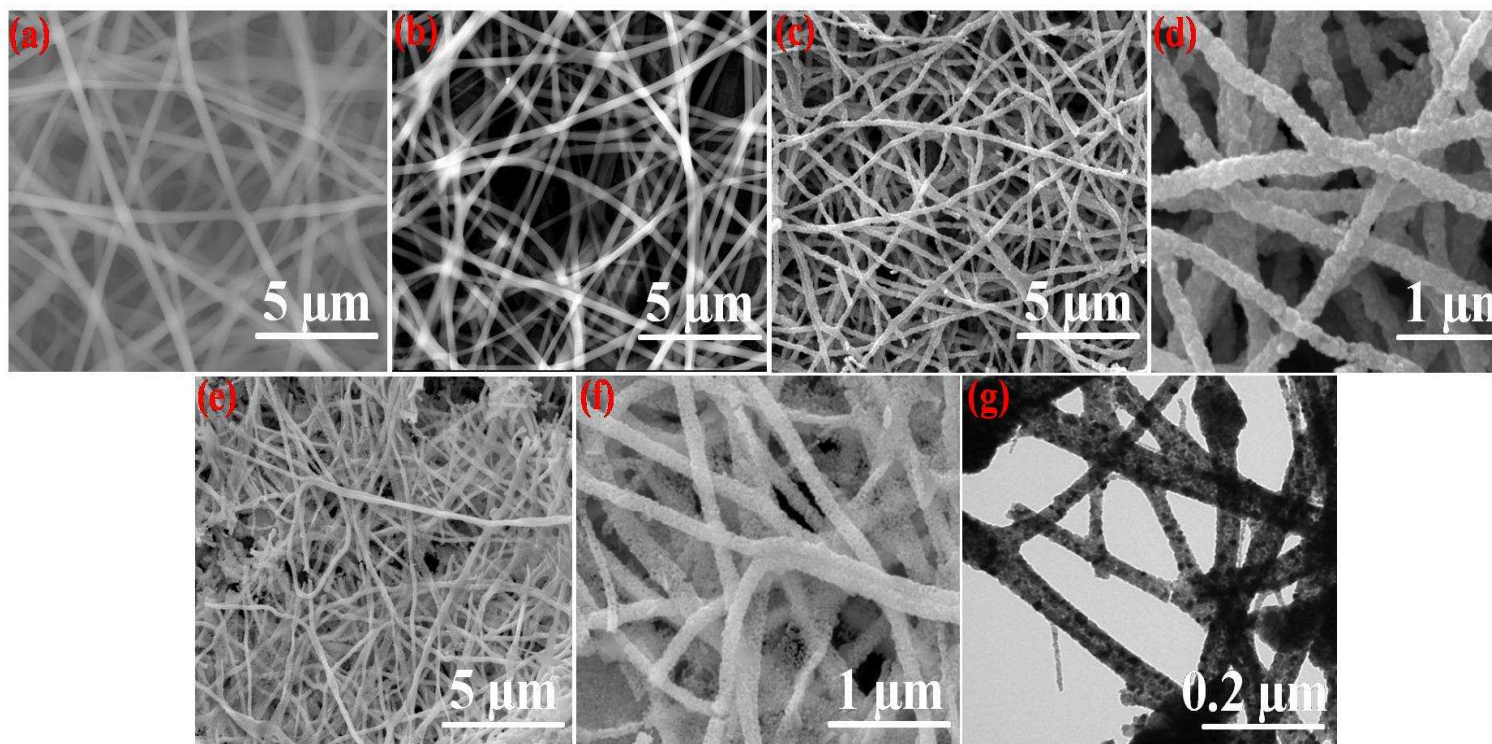


Fig. 1 SEM images of (a) as spun PVA/(Ni(CH₃COO)₂.4H₂O) nanofibers, (b) as spun PVA/(Co(NO₃)₂.6H₂O)/(Ni(CH₃COO)₂.4H₂O) nanofibers, (c,d) annealed bare NiO nanofibers (e,f) annealed Co₃O₄/NiO composite nanofibers and (g) TEM image of annealed Co₃O₄/NiO composite nanofibers.

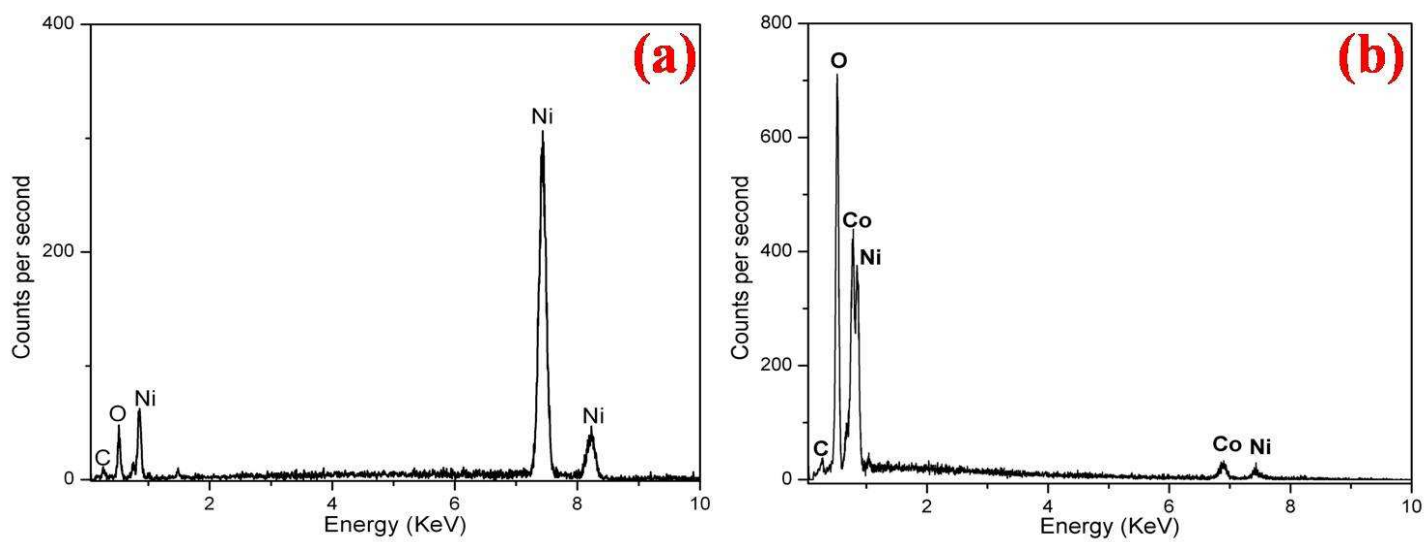


Fig. 2 EDAX patterns of (a) bare NiO and (b) Co₃O₄/NiO composite nanofibers.

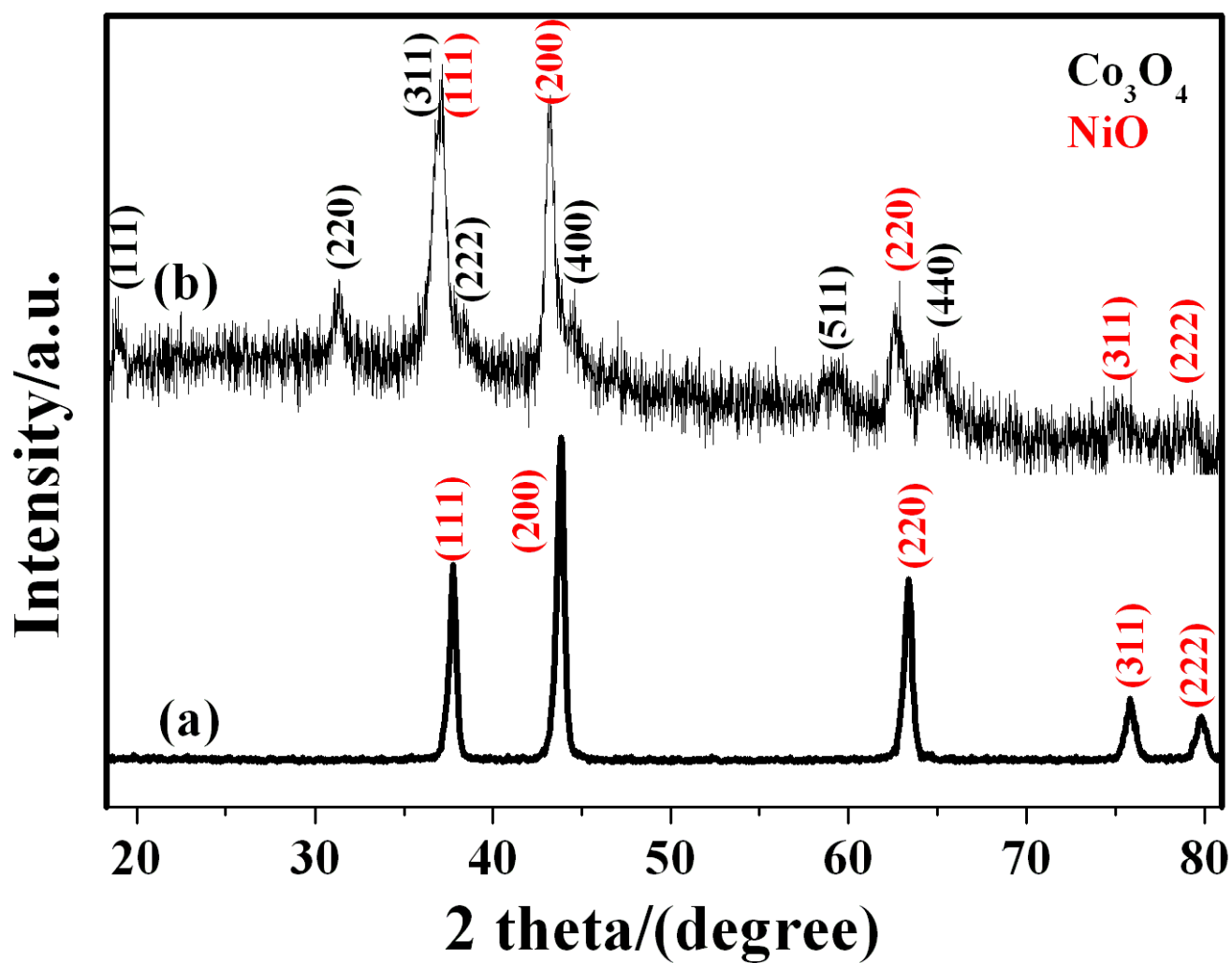


Fig. 3 XRD patterns of (a) bare NiO and (b) Co₃O₄/NiO composite nanofibers.

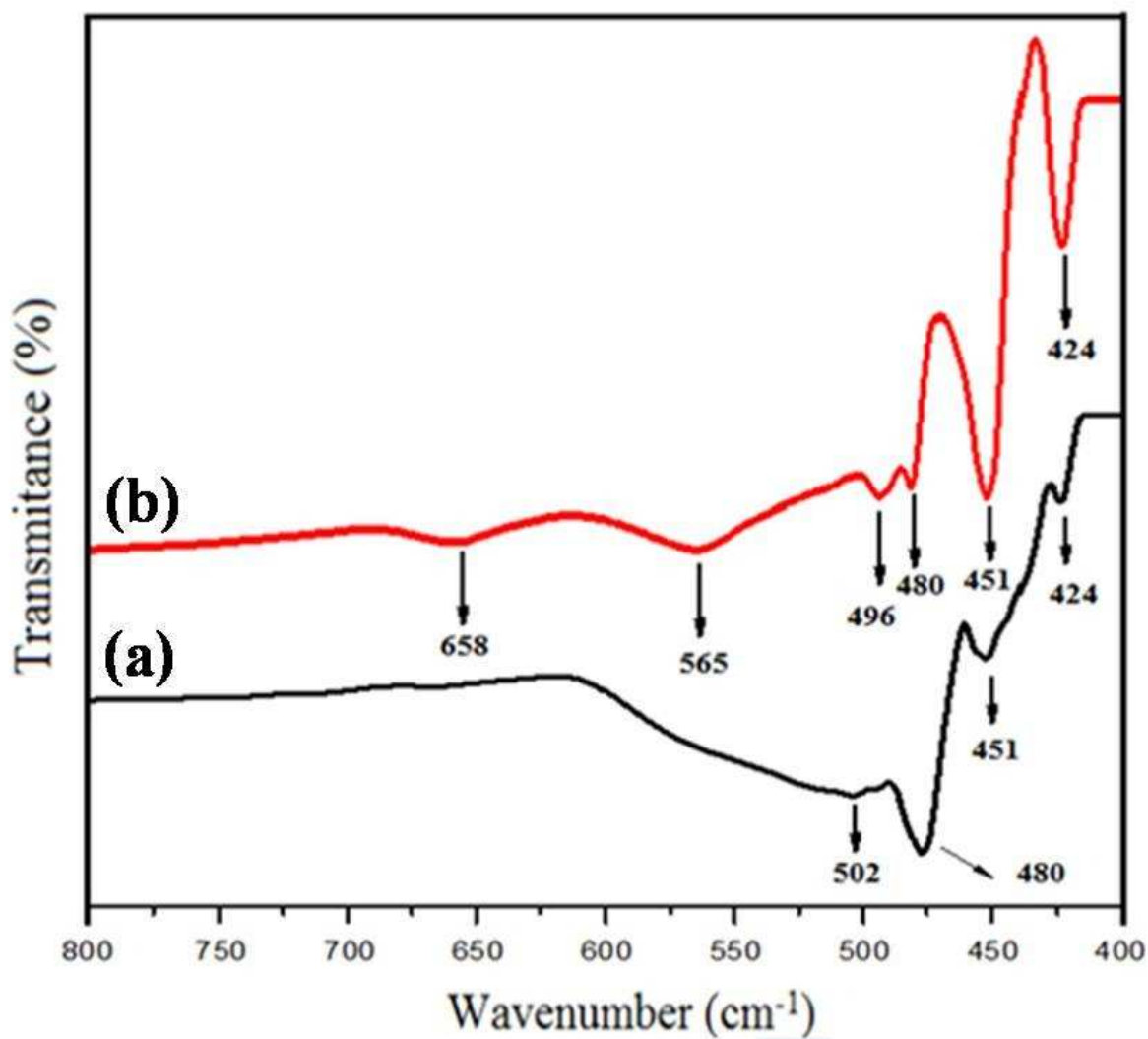


Fig. 4 FT-IR spectra of pure (a) NiO and (b) $\text{Co}_3\text{O}_4/\text{NiO}$ composite nanofibers.

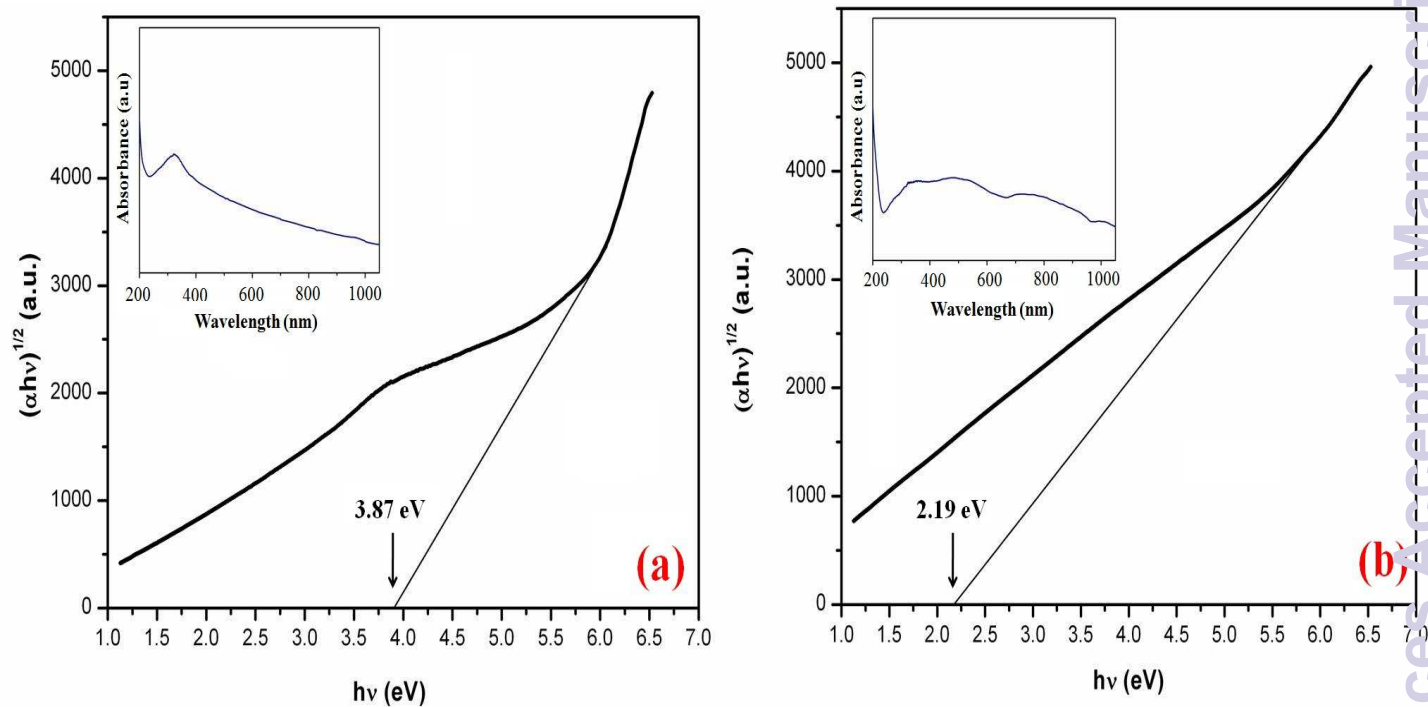


Fig. 5 The optical band gap energy of (a) bare NiO (Inset: UV-*vis* absorption spectrum of bare NiO nanofibers) and (b) $\text{Co}_3\text{O}_4/\text{NiO}$ nanofibers (Inset: UV-*vis* absorption spectrum of $\text{Co}_3\text{O}_4/\text{NiO}$ nanofibers).

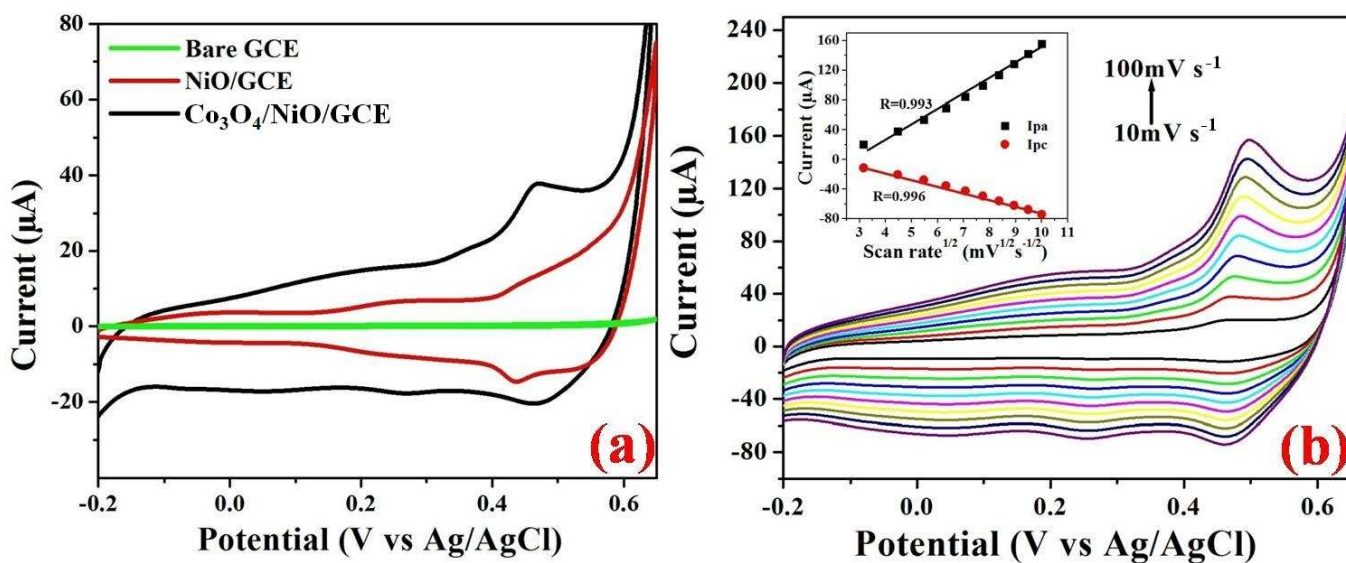


Fig. 6 CVs of (a) studied electrodes in 0.1 M NaOH at a scan rate of 20 mV s^{-1} and (b) $\text{Co}_3\text{O}_4/\text{NiO}/\text{GCE}$ in 0.1 M NaOH as a function of scan rate ranging from 10 to 100 mV s^{-1} (Inset: calibration plot of current vs square root of scan rate).

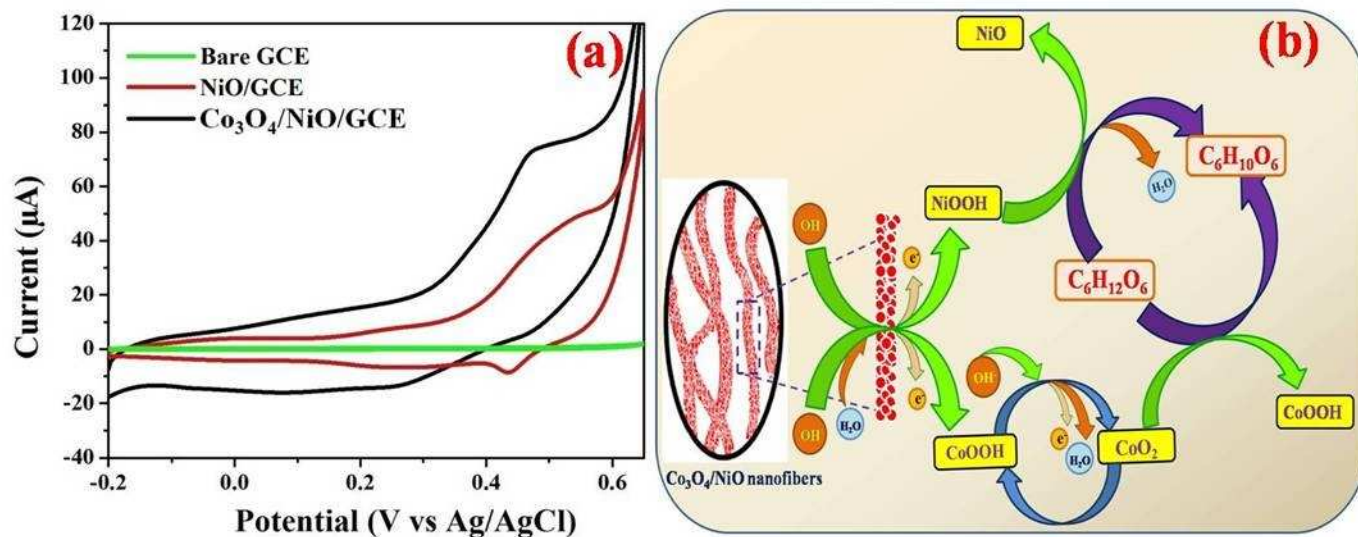


Fig. 7 (a) CVs of studied electrodes under the presence of 1 mM glucose in 0.1 M NaOH at a scan rate of 20 mV s⁻¹ and (b) Mechanism proposed for the electrocatalytic oxidation of glucose at Co₃O₄/NiO nanofibers.

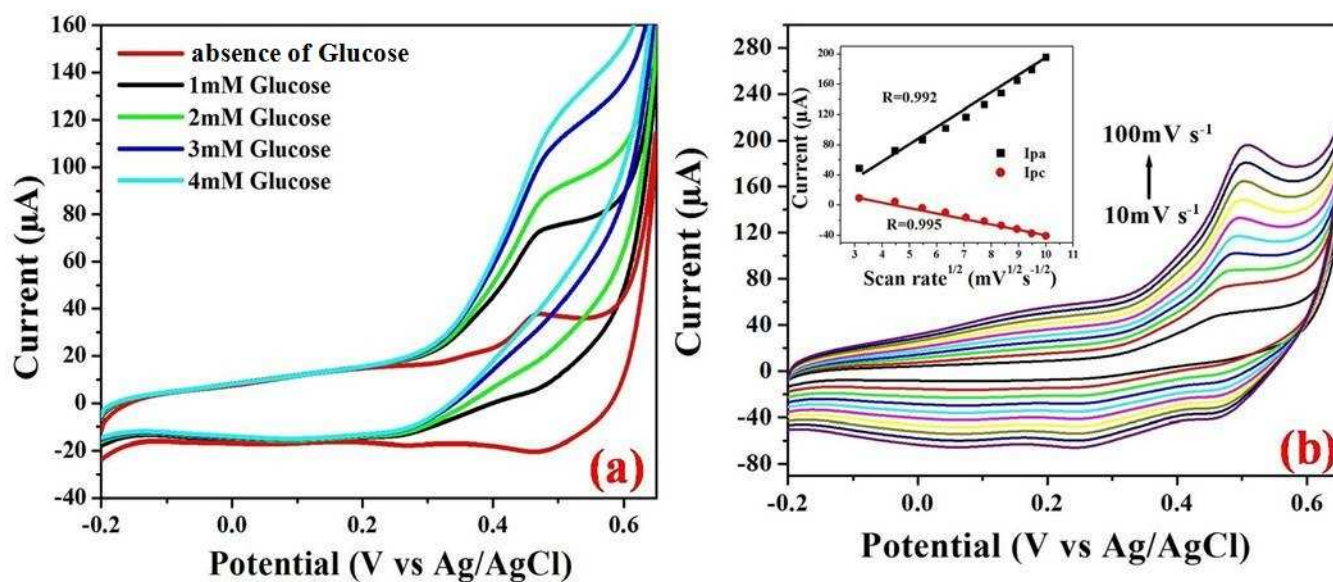


Fig. 8 Cyclic voltammograms of (a) $\text{Co}_3\text{O}_4/\text{NiO}/\text{GCE}$ as a function of glucose concentration in 0.1M NaOH at a scan rate of 20 mV s^{-1} and (b) $\text{Co}_3\text{O}_4/\text{NiO}/\text{GCE}$ in 1 mM glucose in 0.1 M NaOH as a function of scan rate ranging from 10 to 100 mV s^{-1} (Inset: calibration plot of current vs square root of scan rate).

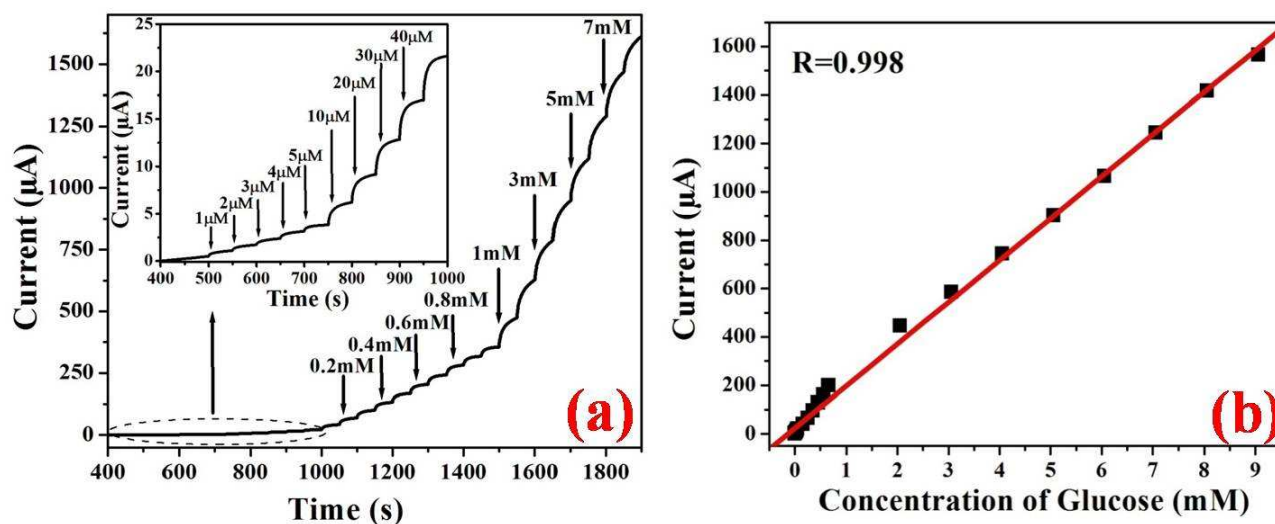


Fig. 9 (a) Amperometric *i-t* responses of Co₃O₄/NiO/GCE with the successive addition of different concentrations of glucose in 0.1 M NaOH solution at an applied potential of 0.5 V vs. Ag/AgCl (Inset: magnified amperometric responses of Co₃O₄/NiO /GCE at initial time) and (b) calibration plot of Co₃O₄/NiO/GCE amperometric responses as a function of glucose concentration.

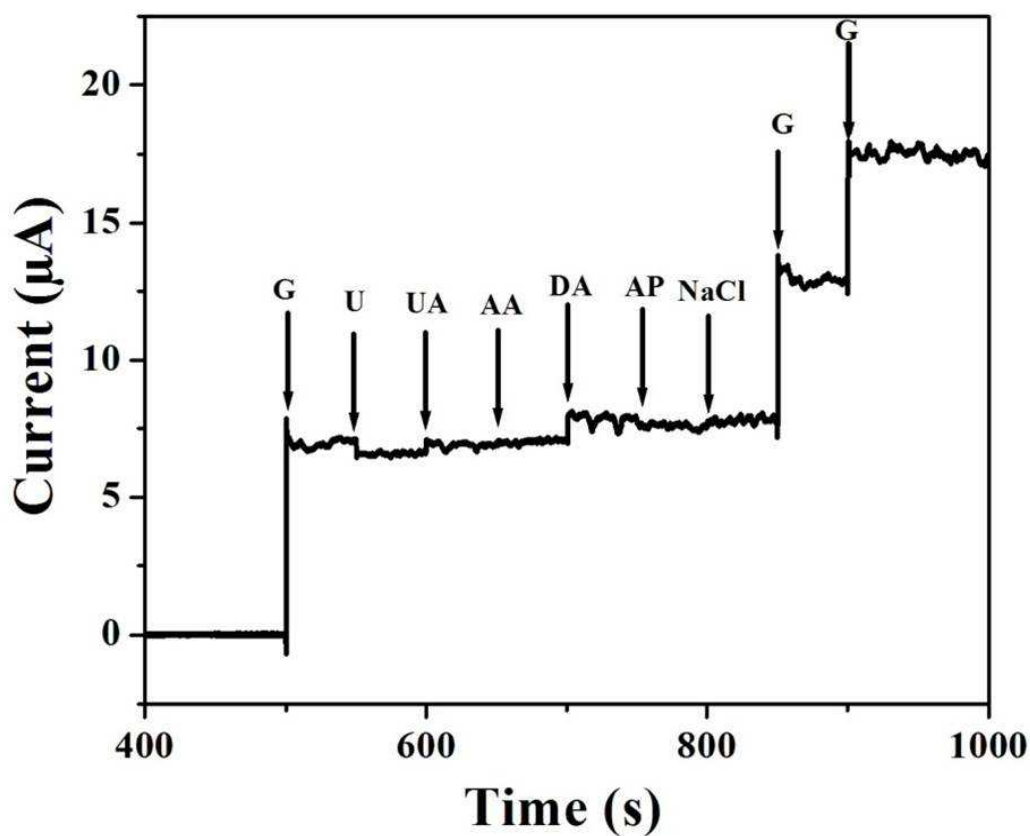


Fig. 10 Selectivity study of $\text{Co}_3\text{O}_4/\text{NiO}/\text{GCE}$ with the successive addition of 1 mM glucose (G), U, UA, AA, DA, AP and NaCl in 0.1 M NaOH at an applied potential of +0.5 V vs. Ag/AgCl.

Table 1 : Comparison of the electrochemical performances of non-precious metal and metal oxide based nanostructures based non-enzymatic glucose sensors.

Electrode material	Sensitivity ($\mu\text{A mM}^{-1}\text{cm}^{-2}$)	Linear range (μM)	LOD^a (μM)	Reference
NiO/MWCNTs ^b	1768.8	10-7000	2	47
CuO NFs ^c	431.3	6-2500	0.8	48
NiO/OMC ^d	834.8	2-1000	0.65	49
NiO/C	582.6	up to 2600	2	50
Ni NWAs ^e	1043	0.5-7000	0.1	51
Ni-Cu/TiO ₂ NTs ^f	1590.9	10-3200	5	52
Pt/Ni NWAs ^e	920	2-1000	1.5	53
NiO-SWCNT ^g	907	1-1000	0.3	54
Ni NP ^h /SMWNTs ⁱ	1438	1-1000	0.5	55
Co ₃ O ₄ NFs ^c	36.25	up to 2040	0.97	56
Ni NP ^h /TiO ₂ NTs ^f	700.2	4-4800	2	57
Ni foam	-	50-7350	2.2	58
Co ₃ O ₄ /NiO NFs ^c	2477	1-9.055	0.17	This work

a-limit of detection; b- multi-walled carbon nanotubes; c-nanofibers; d- ordered mesoporous carbon; e-nanowire arrays; f-nanotubes arrays; g-single-walled carbon nanotubes; h- nanoparticles; i-straight multi-walled carbon nanotubes

Table 2 Determination of glucose concentrations in human serum samples at Co₃O₄/NiO/GCE.

Sample	Glucose added (μM)	Glucose found (μM)	RSD^a (%)	Recovery (%)
1	5	5.2	2.67	104.00
2	10	9.7	3.22	97.00
3	15	15.3	2.85	102.00
4	20	19.6	3.17	98.00
5	25	25.4	3.36	101.60